Interpretation of 1-D Counter-Current Spontaneous Imbibition Processes Using Microscopic Diffusion Theory and a Modified Buckley – Leverett Approach

D. C. Standnes[1], P. Ø. Andersen[1,2], P. Papatzacos[3], and S. M. Skjæveland[1,2]

Affiliations

1 Department of Energy Resources, University of Stavanger, 4036 Stavanger, Norway

2 The National IOR Centre of Norway, University of Stavanger, 4036 Stavanger, Norway

3 Department of Mathematics and Physics, University of Stavanger, 4036 Stavanger, Norway

Corresponding author: Dag Chun Standnes (dcstandnes@yahoo.com)

ABSTRACT

This paper presents a new convenient and easy-to-use method to analyze and calculate measurable quantities in 1-D counter-current (COUC) spontaneous imbibition (SI) processes. Cumulative water imbibed vs time can be calculated both up to and after the water has contacted the no-flow boundary as well as the time required to contact the no-flow boundary. The model's applicability for the whole process is a big advantage compared to other models which only are valid before this event. The method is developed based on a hypothesis that a frontal advance equation (FAE) also can be established for 1-D COUC SI processes in line with the Buckley – Leverett method for forced water imbibition. A relationship between distance travelled, x, by a diffusing water saturation, S_w, and time of the form, $x \sim \sqrt{D(S_w)t}$, is identified from microscopic theory for diffusion. The proportionality factor between distance and time is the square root of the capillary diffusion coefficient, assumed to be constant for a given water saturation, S_w. The corresponding cumulative water volume diffusing into the medium for the same water saturation, S_w, is calculated from the diffusion equation using the same constant capillary diffusion coefficient $D(S_w)$. The final step to establish the FAE is to recalculate the cumulative volume of water imbibed to an equivalent distance (ED) waterfront, i.e. the distance travelled by the imbibing water phase having the same cumulative volume water imbibed as calculated from the diffusion equation. The FAE is similar to the water saturation characteristics in the BL method. The results for cumulative water imbibed vs. time is giving a highly accurate approximation when compared to analytical solutions (i.e. the McWhorter and Sunada solution), deviating slightly from the correct value due to the use of constant diffusion coefficients. The difference can be corrected by a factor in the range 1.0-1.24 for the four datasets considered. The conclusion obtained by comparing the FAE method result to the only experiment dataset in the literature where all input data are available GVB-3 (Bourbiaux and Kalaydjian, 1990), is that the new FAE cannot be falsified within the input parameter uncertainty range. The FAE method is qualitatively corroborated by the results from four 1-D COUC SI cases using synthetic input data as well comparison with many other test results reported in the literature.

1. INTRODUCTION

1.1. Background and Aim. Spontaneous imbibition (SI) of a wetting fluid phase (simply referred to as water) into a porous medium saturated with a non-wetting phase (simply referred to as oil but gas is also occurring herein) takes place due to capillary action on the pore level[1-3]. The non-wetting phase can in general be any non-aqueous phase liquid not miscible with the aqueous phase. The curvature of the non-wetting/wetting interface is decreasing upon increasing volume fraction (saturation) of the imbibing wetting phase such that the chemical potential of the total system decreases towards a fluid saturation distribution where the average curvature of the water – oil interface is zero. The process is spontaneous without any influence of external potentials so the reduction in internal chemical potential

on the way towards equilibrium is balanced by viscous dissipation in the flowing fluids. SI can occur in two different flow modes referred to as co-current and counter-current (COUC). In the former, the imbibing water and displaced oil are moving in the same direction whereas in the latter case, both phases are always moving in opposite direction. COUC SI is an important process[1-26] occurring in nature and in many technical processes ranging from extraction of crude oil from subterranean reservoirs, transfer of ink to paper in printers and the use of porous media for clean-up, absorption of non-aqueous phase liquid, CO_2 sequestration and the relative movement of water and air in soils.

We briefly describe the main features related to 1-D COUC SI test which is the focus of this work. Tests are normally performed using oil as the non-wetting phase and water as the wetting phase[2,11-16] according to the set-up in Fig. 1. Many papers also report experiments where gas was used as the non-wetting phase[17-20]. Some researchers have also used oil as the imbibing wetting phase together with air as the non-wetting phase[19]. The main modelling assumptions related to the 1-D COUC SI setup in the literature and in this work are as follows: The geometry considered is a horizontal rock sample with no-flow boundaries both opposite the entry face and laterally meaning that the imbibing water always is flowing in the opposite direction of the expelled oil. The porous medium is assumed homogenous with constant porosity and absolute permeability. The fluids as well as the rock are considered incompressible and the fluids totally immiscible. All cases are assumed to take place under isothermal conditions, so the fluid viscosities and densities, interfacial tensions and rock wettabilities are constant throughout the process. It is furthermore assumed that the rock sample is initially saturated with a high fraction of the non-wetting phase equivalent to a water saturation, S_{wi}, is totally submerged in the wetting phase at $t = 0$. Hence, the spontaneous flow of wetting phase into the porous medium is taking place in such a way that the volume of wetting phase imbibed exactly equals the non-wetting phase expelled out due to the incompressibility conditions mentioned above. The height of the rock sample is assumed short, so the impact of gravity is assumed negligible. The water saturation in the porous medium when the capillary forces have vanished is S_s. It will be assumed for simplicity that this saturation is identical to maximum mobile water saturation ($1 - S_{or}$), as obtained after a subsequent forced displacement.

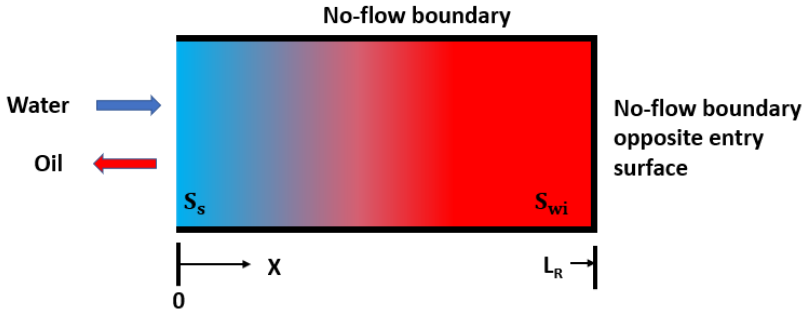

Figure 1. Geometry for the 1-D counter-current spontaneous imbibition process where water is imbibing through the open boundary from left to right expelling oil the opposite way. The initial water saturation is S_{wi} and final saturation after SI has ceased is S_s. The length of the rock sample from the entrance face to the no-flow boundary is L_R and the cross-sectional area is A_{CR}.

In all tests, cumulative water imbibed or as a fraction of maximum water imbibed typically increases proportional to square root of time until the water contacts the no-flow boundary at which time the cumulative water imbibed rate decreases significantly. That is, cumulative volume of water or expressed as fraction of maximum water imbibed (or fractional recovery of non-wetting phase) is a straight line when plotted vs. square root of time during the pre-contact period. It is important to note that the fraction of cumulative water imbibed when the imbibing water first contacts the no-flow boundary typically is in the range from approximately 0.7 (absolute saturation value) and above for very strongly water-wet porous media[18,19,21-26]. The fractional volume imbibed is even higher, close to unity, if gas is used as the non-wetting phase due to its very low viscosity causing an almost piston-like displacement of this phase

by water[18]. Deviation from the straight line when plotting fractional volume of water imbibed vs. square root of time is observed when the water contacts the no-flow boundary, whereupon the rate of water imbibition is significantly reduced. The time required for the imbibing water phase to contact the no-flow boundary and the corresponding water saturation in the rock sample at that time, are two very important quantities in 1-D COUC SI tests since they are directly measurable. The period required to expel the remaining non-wetting phase in the post-contact period can be considerable compared to the time required to transport the imbibing water to the no-flow boundary.

The theoretical models developed to describe 1-D COUC SI, all suffer from the limitations that they only are valid up to the point when the imbibing waterfront contacts the no-flow boundary. This also includes the method developed by McWhorter and Sunada[9] (MS) based on McWhorter[10], recently improved by Schmid and Geiger[6]. This solution has become the standard for the two-phase 1-D COUC SI process with some recent significant improvement in terms of boundary condition interpretation[6] and numerical solution efficiency[27]. Specifically, the MS approach assumed a boundary condition for the inlet water flux q_w as $q_w(x = 0, t) = At^{-\frac{1}{2}}$ where A is a constant. This assumption is still valid even for non-linear diffusion[28] for the initial and boundary condition for the 1-D COUC SI process. Schmid et al.[29] showed that this condition was not a restriction, but consistent with the mathematical equations and fixed saturation boundary condition used to model COUC SI. They derived an effective fractional flow function $F(S_w)$ such that each saturation was displaced with time given by $x(S_w) = \frac{2A}{\phi}F'(S_w)t^{\frac{1}{2}}$ and the cumulative imbibed water Q_w was then given by $Q_w(t) = 2A_{CS}At^{\frac{1}{2}}$. Here A_{CS} is the cross-sectional area of the medium. $F(S_w)$ can be calculated from an implicit integral equation involving $D(S_w)$, while A then can be calculated from $F(S_w)$ (see APP. for a description of the algorithm used). Other authors have also provided solutions under different conditions[11,30-33] or by simulations[34-36]. A semi-analytical method was developed by Abd et al.[1], where the square root of time scaling was proposed ad hoc to derive an equation to describe counter-current imbibition numerically. More sophisticated models for COUC SI also accounting for non-equilibrium effects have been proposed, see e.g.[23,37]. Now, the phenomenon of diffusion is per definition a non-equilibrium process driven by gradients in chemical potential and quantified by the magnitude of the diffusion coefficient. For the case of imbibition, changes in chemical potential are caused by reduction of interfacial energy stored in the oil-water interface originally established by applying external energy to the system (a drainage process). It is therefore assumed herein that standard diffusion theory is applicable to describe the spontaneous imbibition process until empirical data indicate otherwise (principle of Occam's razor).

The aim of the current paper is to present a new convenient and easy-to-use method referred to as the frontal advance equation (FAE) method to interpret and estimate measurable quantities in 1-D COUC SI processes. These quantities include e.g. cumulative water imbibed vs. time, the time and water saturation when water contacts the no-flow boundary and the decline in rate of imbibition in the post-contact period. The new FAE method is developed based on that 1-D COUC SI is described by a diffusion-like equation and the hypothesis that a FAE can be identified for this process in line with the Buckley – Leverett (BL) method for forced imbibition[38]. The method bears similarity to the MS method, i.e. there should be a function G such that $x(S_w) = G(S_w)t^{1/2}$. A relationship between distance travelled, x, by a diffusing substance and time can according to microscopic theory for diffusion be expressed as, $x \sim \sqrt{D_M t}$, where D_M is the diffusion coefficient for the actual process considered (see [39] or any other book in statistical physics). For the case of 1-D COUC SI, the relationship becomes, $x \sim \sqrt{D(S_{w0})t}$, in which $D(S_{w0})$ is the capillary diffusion coefficient (see eq. (4) later). The capillary diffusion coefficient, $D(S_{w0})$ appearing in the proportionality factor is assumed to be constant for a given value of the water saturation, S_{w0}. On the other hand, 1-D COUC SI processes are on the macroscopic level (see eq. (1) later) described by a diffusion equation with fixed initial and boundary conditions. The solution of the diffusion equation using the fixed diffusion coefficient, $D(S_{w0})$, gives a distribution of imbibing water phase in space and time from which cumulative water imbibed for a particular water saturation, S_{w0}, can be determined analytically by integration. The cumulative water volume for the specific water saturation, S_{w0}, is used to give an equivalent distance (ED) x_{ED}, i.e. the distance travelled if the saturation profile has the uniform value of the imbibing water saturation S_{w0}.

This provides a characteristic (distance-time relation with constant saturation) for each mobile saturation with a positive capillary pressure. Hence, the FAE concept is equivalent to the water saturation characteristics concept used in the conventional BL method. Thus, similar calculation procedures as used for the conventional BL method will also apply when using the FAE for 1-D COUC SI processes. Especially, a front saturation is derived from mass conservation and a continuous saturation profile behind the front is produced. The time to reach the no-flow boundary is estimated. The model is also used to assess the development of the water saturation profile after the waterfront has contacted the no-flow boundary based on BL principles assuming that each characteristic travel undisturbed until it reaches the no-flow boundary. The semi-analytical MS method will be used for reference to calculate exactly the cumulative water imbibed vs. time in 1-D COUC SI process. Due to the proportionality with square root of time (of both profiles and production), a correction factor can be introduced to bring our presented approximate solution in complete agreement with the exact solution.

The rest of the paper is organized in the following way. Following this subsection, another subsection follows which describes in more detail the idea, hypothesis and framework related to the FAE concept. The theory section follows where all details about the FAE method development will be outlined. In the Results and Discussion section, results from using the FAE method for four synthetic dataset cases will be presented. Additionally, the FAE method will be used to match experimental 1-D COUC SI behavior for the only complete datasets in the literature where all input data are available for model testing and comparisons (Bourbiaux and Kalaydjian[12]). The status of the main hypothesis will be assessed therefrom, falsified/corroborated. A discussion of the main uncertainties related to the new FAE method is presented in the discussion before the conclusions from the work is listed in the last paragraph.

1.1 Mathematical formulation of the 1-D COUC SI problem. The problem we wish to solve is the nonlinear diffusion equation:

$$\frac{\partial S_w}{\partial t} = \frac{\partial}{\partial x}\left(D(S_w)\frac{\partial S_w}{\partial x}\right) \quad (1)$$

with initial condition: $S_w(x, t = 0) = S_{wi}$ (2)

and boundary conditions:

$$S_w(x = 0, t) = S_S \qquad \partial_x S_w = 0 \text{ at } (x = L_R) \quad (3)$$

In the above, S_w is water saturation, t time, x spatial coordinate and $D(S_w)$ the capillary diffusion coefficient given by:

$$D(S_w) = -\frac{K}{\phi}\frac{k_{ro}}{\mu_o} f(S_w)\frac{dP_c}{dS_w} \quad (4)$$

Here K is absolute permeability, ϕ porosity, k_{ro} relative permeability to oil, μ_o oil viscosity and P_c capillary pressure conventionally defined as the pressure in the oil phase minus pressure in the water phase. Furthermore, $f(S_w)$ is the fractional flow function known from BL two-phase displacement theory given by:

$$f(S_w) = \frac{\frac{k_{rw}}{\mu_w}}{\frac{k_{rw}}{\mu_w} + \frac{k_{ro}}{\mu_o}} \quad (5)$$

where k_{rw} is relative permeability to water and μ_w water phase viscosity.

1.2. Idea, Hypothesis and Method Framework. A major feature of the BL method is that it can quantify the development of the water saturation in a confined oil reservoir, initially containing oil and water, throughout the whole process. Water is injected into the reservoir and oil and water can be produced from a production well. 100 % oil is produced until water breakthrough occurs. The water saturation in the production well at water breakthrough is equal to the water shock front saturation. The BL method

can additionally quantify the development of the oil and water production after water breakthrough to the point in time where only water is produced. This is possible since the BL frontal advance equation given as,

$$x = \frac{q}{A_{CS}\phi}\left(\frac{df}{dS_w}\right)\cdot t \qquad (6)$$

describes the distance each water saturation is moving along each water saturation characteristic vs. time. Since each water saturation characteristic is moving with its own velocity, the arrival time and hence the development of the water saturation in the production well can be calculated at any point in time. It should be noted that the injected water and displaced oil are moving in the same direction, so-called co-currently, when considering forced imbibition. In eq. (6), x is the position of a particular water saturation characteristic at time t, A_{CS} the cross-sectional area of the reservoir, q is water volume injection rate and $\left(\frac{df}{dS_w}\right)$ is the dimensionless velocity for a given water saturation.

The FAE method developed in this paper is based on the idea that the phenomenon of diffusion, i.e. spreading of matter caused by gradients in the chemical potential, on the microscopic level is described by Brownian motion theory. From this theory, the mean displacement of a diffusing Brownian particle is given by[39],

$$x \sim \sqrt{2D_M}\cdot\sqrt{t} \qquad (7)$$

Here, D_M is the diffusion coefficient for the process considered and it determines the propagation velocity of the diffusing substance. It is therefore hypothesized that eq. (7) can be used to establish a relationship between distance travelled and time for a 1-D COUC SI process in line with the BL frontal advance equation (eq. (6)), although the dependency in eq. (7) is proportional to square root of time instead of time. The idea is that the distance travelled by a given water saturation in a 1-D COUC SI setting is given by the magnitude of the corresponding capillary diffusion coefficient evaluated at that water saturation. In the BL method, the distance travelled by the water saturation is proportional to the dimensionless velocity, $\left(\frac{df}{dS_w}\right)$. In analogy, the distance travelled by the water saturation in 1-D COUC SI is proportional to the square root of the capillary diffusion coefficient, $D(S_w)$. The main gain by establishing an analogy to the BL method is that the new FAE method will describe the development of water saturation for all times. Furthermore, well-established BL calculation procedures are immediately available to calculate cumulative water imbibed vs. time throughout the whole SI process.

Now, eq. (7) describes the relationship between distance travelled and time for a substance diffusing with a diffusion coefficient D_M. To quantify the relationship between distance travelled and the cumulative volume of water imbibed, a relationship between cumulative water imbibed and time is required. 1-D COUC SI obeys a diffusion-type equation[4,6,35,40,41] on the macroscopic level with appropriate initial and boundary conditions given by eqs. (1)-(3). Eq. (1) describes non-linear diffusion since the capillary diffusion coefficient $D(S_w)$ given in eq. (4) obviously is depending on water saturation through the saturation dependent flow functions[41] k_{rw}, k_{ro} and $\frac{dP_c}{dS_w}$. The idea now is to use the diffusion equation in eq. (1) to calculate cumulative water imbibed into the porous medium for each water saturation in the mobile saturation range. Because eq. (1) is non-linear, its solution can only be given semi-analytically by e.g. the MS solution procedure. To obtain an analytical expression for cumulative water imbibed where the relationship between all parameters involved is shown explicitly, the linear version of eq. (1) (constant capillary diffusion coefficient) will be used since an analytical solution exists for this case. The use of a constant diffusion coefficient evaluated for each separate water saturation S_{w0} such that, $S_{wi} < S_{w0} < S_S$, is evaluated to give explicit solutions which are recombined to give a solution to the general problem eq. (1). The details are explained in the next section. As will be seen this approach gives quite accurate results for cumulative water imbibed but induces an error compared to the exact solution which depends on the shape of the capillary diffusion coefficient vs. water saturation. Hence, a correction factor N will be introduced to bring the cumulative water imbibed according to the new FAE method in complete agreement with the exact water volume imbibed calculated using the MS solution procedure, if accurate results are required.

2. DEVELOPMENT OF FRONTAL ADVANCE METHOD TO INTERPRET 1-D COUNTER-CURRENT SPONTANEOUS IMBIBITION PROCESSES

The main development steps of the solution procedure will be outlined in these sections. The development of the new FAE method comprises two main steps. We first establish a new characteristic, i.e. a functional relation between distance and time for a specific water saturation. This will be based on the mean distance x_{ED} water would have diffused with fixed inlet saturation S_{w0} and constant diffusion coefficient $D(S_{w0})$. These combined saturation vs. distance profiles give explicit expressions for cumulative water volume imbibed, saturation profile and front, breakthrough time and behavior before and after reaching the boundary. In other words, a FAE for 1-D COUC SI processes.

2.1. The Relationship between Distance Travelled, Volume Imbibed, Equivalent Distance and the Capillary Diffusion Coefficient.

Diffusion processes are fundamentally the consequence of molecular level processes which can be described phenomenological on the microscopic level by Brownian motion theory[42-44]. Hence, eq. (7) above gives the relationship between a representative distance travelled, $x(t, S_{w0})$, for a specific water saturation value, S_{w0}, diffusing into a porous medium as a function of time as,

$$x(t, S_{w0}) = C\sqrt{D(S_{w0})t} \tag{8}$$

Displacement length, x, is here only a function of time since the value of $D(S_{w0})$ is determined for a given fixed value of the water saturation S_{w0}. C is a proportionality factor which will be determined later. Hence, distance travelled, $x(t, S_{w0})$, by each water saturation in the mobile water saturation range assumed to be in the range from $S_{wi} = 0.2$ to $S_s = 0.68$ herein where $D(S_{w0}) \geq 0$, is proportional to respective values on the curve given in Fig. 2. Now, to calculate analytically cumulative water imbibed into the porous medium for each water saturation, S_{w0} in the range from S_{wi} to S_S, the linear version of the diffusion eq. (1) will be used given as,

$$\frac{\partial S_w}{\partial t} = D(S_{w0})\frac{\partial^2 S_w}{\partial x^2} \tag{9}$$

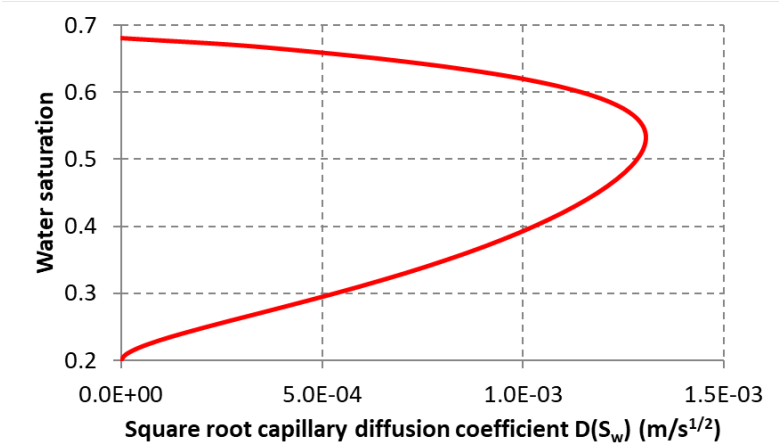

Fig. 2. Mobile water saturations 0.2 – 0.68 plotted vs. square root of the capillary diffusion coefficient defined by eq. (4).

The analytical solution to eq. (9) describes how the water saturation, $S_w(x, t)$, varies in space and time away from a source with constant fixed water saturation value, S_{w0}, higher than the initial water saturation, S_{wi}. It is given as a complementary error function (erfc)[28],

$$S_w(x,t) = (S_{w0} - S_{wi}) \cdot \mathrm{erfc}\left(\frac{x}{2\sqrt{D(S_{w0})t}}\right) + S_{wi} \qquad (10)$$

For known $D(S_{w0})$, eq. (10) describes water saturation vs. distance from the source for different times as illustrated in Fig. 3. This example has, for simplicity, maximum water saturation $S_S = 1$ and initial water saturation, $S_{wi} = 0$. Cumulative water imbibed into the medium increases with time and a final water saturation of $S_w = 1$ will be obtained everywhere after a very long period. Using the properties of self-similarity could gather these profiles to one, but do not add any advantage when combining the contributions from solutions originating from different S_{w0} since each water saturation has a corresponding diffusion coefficient different in magnitude. Also, the relationship to the BL procedure is a major point of the current work.

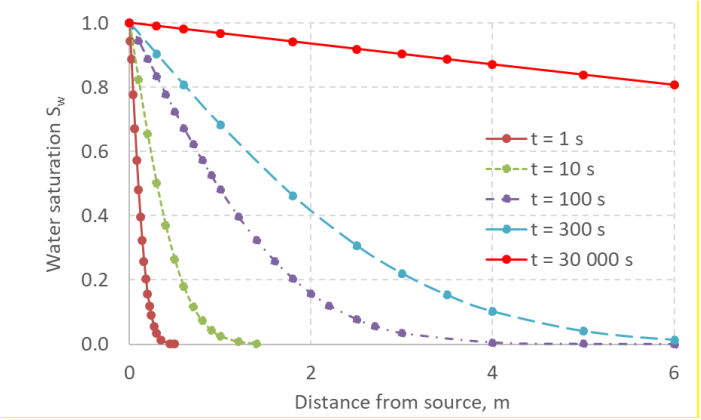

Figure 3. The analytical solution (eq. (10)[28]) to linear 1-D COUC flow of water and non-wetting phase showing water saturation vs. distance from the source located on the y-axis for different times. Input parameters: $D(S_{w0}) = 0.01\mathrm{m}^2/\mathrm{s}$, $S_S = 1$, $S_{w0} = 1$ and $S_{wi} = 0$.

Having an analytical expression for variation of water saturation in space and time (eq. (10)) allows for determination of cumulative water imbibed under the assumption of constant diffusion coefficient evaluated for each water saturation, S_{w0}. It is given as the area under the water saturation profiles above the initial saturation, as shown in Fig. 3. The area can be found by integrating the water saturation profile in eq. (10) analytically from distance zero to infinite. In the expression below, A_{CS}, is the cross-sectional area of the porous medium perpendicular to the saturation profile. Hence,

$$\text{Cumulative volume water imbibed} = A_{CS}\int_{x=0}^{\infty} S_w(x)dx$$

$$= A_{CS}\int_{x=0}^{\infty}(S_{w0} - S_{wi}) \cdot \mathrm{erfc}\left(\frac{x}{2\sqrt{D(S_{w0})t}}\right)dx$$

$$= A_{CS}(S_{w0} - S_{wi})\left[x \cdot \mathrm{erfc}\left(\frac{x}{2\sqrt{D(S_{w0})t}}\right) - 2\sqrt{D(S_{w0})t}\,\frac{e^{-\frac{x^2}{4D(S_{w0})t}}}{\sqrt{\pi}}\right]_0^{\infty} = A_{CS}\frac{2(S_{w0}-S_{wi})\sqrt{D(S_{w0})t}}{\sqrt{\pi}} \qquad (11)$$

As shown in Fig. 3, diffusive processes are featured by spreading of e.g. particles or water out in space from a source as a function of time. The source has a constant value equal, S_{w0}, throughout the process for the cases studied. Hence, the displacement length referred to above, $x(t, S_{w0})$ in eq. (8), is therefore not a well-defined quantity. To obtain well-defined water saturation positions for each diffusing water saturation, S_{w0}, shown in Fig. 3, the cumulative volume of water imbibed vs. time determined from the analytical solution (eq. (10)) will be used to define an equivalent distance (ED) water, x_{ED}, for each water saturation, S_{w0}. This is performed by equating cumulative water volume imbibed determined from eq. (10) at time t to a rectangular step water saturation profile with height

equal to $S_{w0} - S_{wi}$, and width equal to the ED value x_{ED}. This will ensure preservation of volume of water imbibed at all times,

$$x_{ED}(t, S_{w0}) \cdot (S_{w0} - S_{wi})A_{CS} = \frac{2(S_{w0}-S_{wi})\sqrt{D(S_{w0})t}}{\sqrt{\pi}}A_{CS} \quad (12)$$

Hence,

$$x_{ED}(t, S_{w0}) = \frac{2}{\sqrt{\pi}}\sqrt{D(S_{w0})t} \quad (13)$$

so, the proportional factor $C = \frac{2}{\sqrt{\pi}}$ in eq. (8). This calculation is illustrated in Fig. 4 where x_{ED}, is the distance from $x = 0$ to the position $x \approx 1.13$, over which the area with constant saturation height equal to $S_{w0} - S_{wi}$ gives the same area as the area imbibed determined from the diffusive solution (eq. (10)).

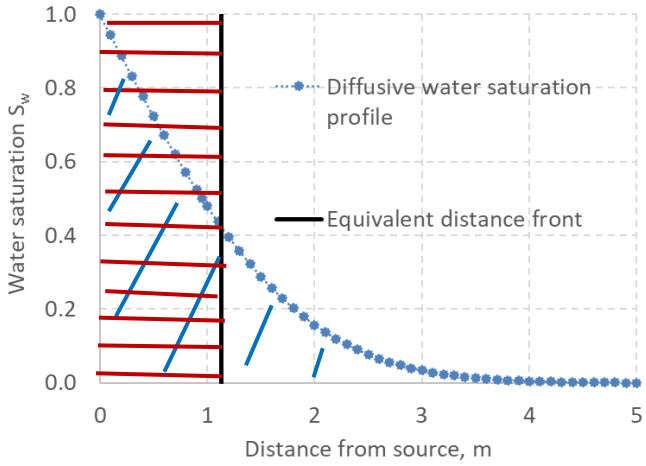

Figure 4. Determination of x_{ED}. The area below the diffusive water saturation profile (eq. (10)), corresponds to cumulative water imbibed at $t = 100$ s (input parameters: $D(S_{w0} = 1) = 0.01$ m^2/s, $S_S = 1$, $S_{w0} = 1$ and $S_{wi} = 0$. The ED, x_{ED}, is the distance from $x = 0$ to the black vertical line at $x_{ED} \approx 1.13$ m determined such that the rectangle, $(S_{w0} - S_{wi})x_{ED}$, has the same area as the blue shaded area below the blue curve.

For each specific water saturation value, S_{w0}, x_{ED} varies according to eq. (13) only with square root of time since the magnitude of $D(S_{w0})$ is fixed for a known given water saturation, S_{w0}. Hence, the ED vs. time, can finally be expressed explicitly substituting the terms in eq. (4) for the capillary diffusion coefficient into eq. (13) so,

$$x_{ED}(t, S_{w0}) = N\frac{2}{\sqrt{\pi}}\sqrt{\frac{K}{\phi}} \cdot \left[\sqrt{\frac{k_{ro}k_{rw}}{\mu_o k_{rw} + \mu_w k_{ro}}} \cdot \sqrt{\frac{dP_c}{dS_w}}\right]_{S_{w0}} \cdot \sqrt{t} \quad (14)$$

where S_{w0} varies in the mobile water saturation range from S_{wi} to S_s. Eq. (14) also contains a correction factor N (independent of S_{w0}) introduced to compensate for the possibility that using a constant diffusion coefficient for each water saturation, S_{w0}, only gives an approximate value for cumulative water imbibed even when combining the contributions from all saturations S_{w0}. The correction factor can, for any case studied be calculated by comparing the combined solution with the exact MS solution where a value of $N = 1$ implies a perfect correspondence. A correlation will be presented later giving values for N depending on the shape of the capillary diffusion coefficient.

Eq. (14) is the key expression established herein as it represents the FAE for 1-D COUC SI processes, analogous to the BL frontal advance equation for forced imbibition (eq. (6)), i.e. it provides a characteristic for a specific saturation such that the position with time of that saturation can be calculated. Since any $x_{ED}(t, S_{w0})$ is proportional to the square root of time, so will any combination of

these solutions which is a result in line with empirical data for 1-D COUC SI of water into oil-saturated porous media[2,6,7,11-14,16,17,19,20,24,29,45-47] where production is seen to follow a root of time behavior. Hence, the square root of imbibition time behavior is not assumed herein as a boundary condition but follows directly from microscopic diffusion theory. Eq. (14) further emphasizes the importance of the capillary diffusion coefficient, $D(S_{w0})$, when considering 1-D COUC SI processes, as it contains all the information required to link the ED, x_{ED}, for each propagating water saturation to imbibition time. All variables in eq. (14) are standard and can be measured independently except the correction factor N appearing because of the assumption of a constant capillary diffusion coefficient. Eq. (14) expresses the location, x_{ED}, for each saturation calculated as described and can be plotted in the range from S_{wi} to S_s at a given time as shown in Fig. 5. This distribution of saturations vs. their ED positions, x_{ED}, presents the combined estimate of the saturation profile and its area (sketched in the figure) equal to the cumulative water imbibed per unit cross-sectional area.

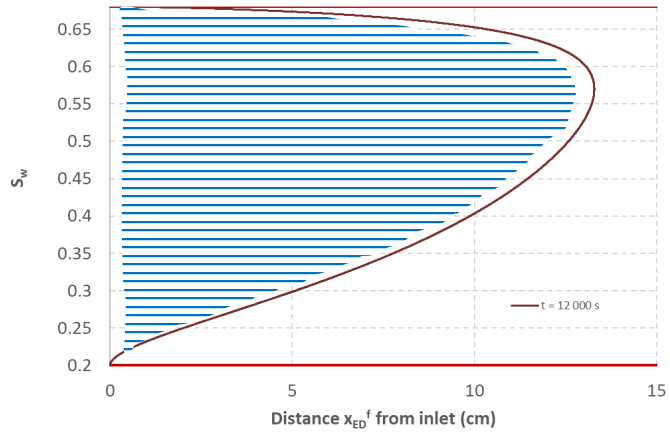

Figure 5. ED water saturations travelled for all water saturations between $S_{wi} = 0.2$ and $S_s = 0.68$ at time t = 12,000 s calculated from eq. (14) with input data given in Table 1 for the SWW case.

Since the FAE (eq. (14)) can give a curve which has a maximum position for an intermediate water saturation (as in Fig. 5), it requires the introduction of an ED water front position, x_{ED}^f, and front saturation S_{SF} since physical arguments require that only one saturation can be present at the same location at the same time. Using the principles of mass (volume) conservation and front velocity equal to the front saturation velocity, as in conventional BL fractional flow analysis[48], we obtain the location x_{ED}^f and saturation S_{SF} of the shock waterfront for 1-D COUC SI. Graphically, this can be performed by ensuring that the two shaded areas in Fig. 6 are equal, where the black curve vertical line represents the ED water front.

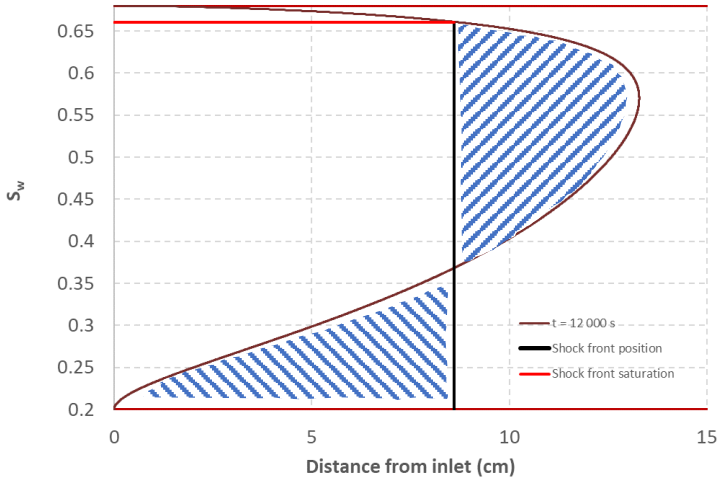

Figure 6. Calculation of ED water front, x_{ED}^{f}, at t = 12,000 s from eq. (14) using input parameters in Table 1 for the SWW case. The front is located such that the two shaded areas are equal. The water saturation behind the ED front increases from the front water saturation, $S_{SF} = 0.66$, up to the maximal water saturation, $S_s = 0.68$.

2.2. Calculation of Cumulative Water Imbibed at Early and Late Times. The idea now is to apply the curve S_w vs. $x_{ED}(S_w)$ to quantify cumulative water imbibed vs. time until the SI process ceases. Additionally, the time required for the water phase to contact the no-flow boundary, t_R, will be determined. Early time (ET) will in the following refer to $t < t_R$ whereas late time (LT) is the period $t > t_R$. At early time (before BT) cumulative (volume) water imbibed, R_{V_ET}, is given by considering the area under the imbibed profile:

$$R_{V\_ET} = A_{CS}N\phi(S_{SF} - S_{wi})x_{ED}^{f} + A_{CS}N\phi\int_{S_{SF}}^{S_S} x_{ED}dS_w \quad (15)$$

Similarly, fraction of maximum cumulative water uptake (R_{ET}), is given by:

$$R_{ET} = N\frac{(S_{SF}-S_{wi})x_{ED}^{f}+\int_{S_{SF}}^{S_S} x_{ED}dS_w}{(S_S-S_{wi})L_R} \quad (16)$$

Introduction of the ED shock front water saturation also allows for calculation of the time, t_R, required for the ED shock front to arrive at the no-flow boundary. Hence, from eq. (14) with water saturation equal to the ED shock front saturation, S_{SF}, gives,

$$t_R = \frac{\pi}{4}\frac{\phi}{K}\frac{L_R^2}{N^2\left[\frac{k_{ro}k_{rw}}{\mu_o k_{rw}+\mu_w k_{ro}}\frac{dP_c}{dS_w}\right]_{S_{SF}}} \quad (17)$$

t_R is a very important quantity related to 1-D COUC SI processes as it is directly measurable. The curve for cumulative water imbibed (or as fraction of water imbibed to the maximum water volume) vs. square root of time is deviating from a straight line when the imbibing water phase contacts the no-flow boundary. Hence, all 1-D COUC SI models should from an empirical point of view, be able to predict both the value of t_R and a water shock front saturation that agrees with the experimentally observed average water saturation.

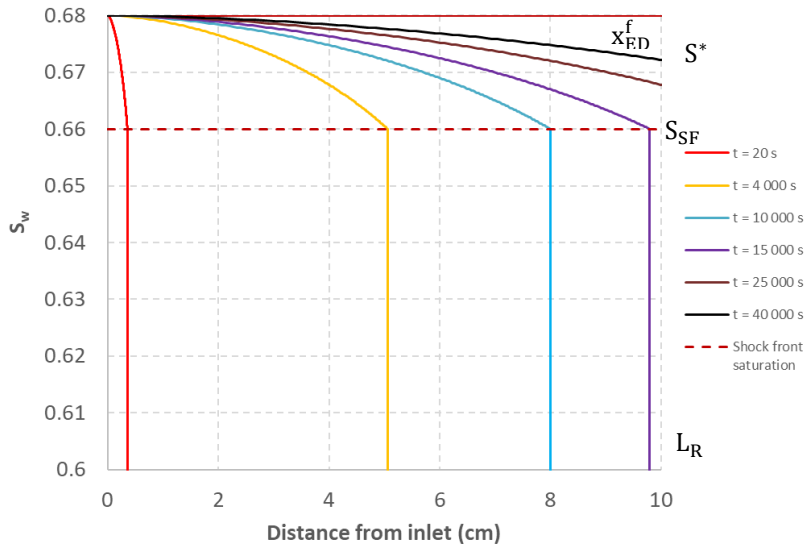

Figure 7. Predicted water saturation profiles at different times (focusing on the saturations above 0.6). $S_{wi} = 0.2$, $S_{SF} = 0.66$ (dotted red horizontal line) and $S_s = 0.68$. Left of the no-flow boundary, saturation profiles with a shock front are depicted at four different times propagating proportionally to the square root of time towards the right. The water saturation at the no-flow boundary L_R after the shock front contacts this boundary is called S^*. The process will continue until S^* equals S_s.

Existing models for 1-D COUC SI cease to be valid when the imbibing water phase contacts the no-flow boundary. Since the BL methodology is assumed to apply for the movement of each water saturation throughout the whole process, cumulative water imbibed in the post-contact period is calculated by assuming that all ED front positions, x_{ED}^f, for water saturations that have not reached the no-flow boundary, continue undisturbed, and stop when they sequentially reach the no-flow boundary. It then follows that cumulative water imbibed for late times (after the ED water shock front has reached the no-flow boundary), R_{V_LT}, is equal to the volume added by the profile of the saturations that have reached the boundary and volume contribution of the remaining saturations that have a continuous profile extending from the boundary,

$$R_{V\_LT} = A_{CS}\phi L_R(S^* - S_{wi})L_R + A_{CS}N\phi \int_{S^*}^{S_S} x_{ED}\,dS_w \qquad (18)$$

Here, S^*, is the highest water saturation located exactly at the no-flow boundary of the porous medium. It is defined as the saturation higher than S_{SF} which has position exactly equal to the no-flow boundary at that time. As the water saturations above the ED shock front saturation continuously arrive at the no-flow boundary, S^* will increase with time, see Fig. 7. The 1-D COUC SI process ceases when S^* finally equals S_S. The fraction of maximum uptake of water during the late time period, R_{LT}, is then given by:

$$R_{LT} = \frac{\left[(S^* - S_{wi})L_R + N\int_{S^*}^{S_S} x_{ED}\,dS_w\right]}{(S_S - S_{wi})L_R} \qquad (19)$$

R_{LT} will be identical to unity when the x_{ED} corresponding to the saturation S_s, has reached L_R. The expressions in eq. (16) and (19) give cumulative water imbibed as a function of time for both early and late time (R_{ET} and R_{LT}), respectively. Hence, expressions for calculating cumulative water imbibed or recovery numbers for the whole 1-D COUC SI process are established. Together with the illustration in Fig. 7 they explain experimentally observed trends of early time square root profiles with time of cumulative water imbibed and late time trends deviating from this as well as observations of front-like displacement from saturation imaging[19-21,23,24,45,46,49-54]. At early times, all water saturations in the range from S_{wi} to S_s are moving with square root of time, hence so does cumulative water imbibed. In the period after the ED shock front contacts the no-flow boundary, the only water saturations moving and

contributing to increased water saturation in the medium are those with value higher than the ED shock front saturation. The saturations in the range S_{wi} to S^* no longer contribute since they already have reached the no-flow boundary. But since the range of saturation with distances x_{ED}^f traveling towards the no-flow boundary is decreasing with time, the cumulative water imbibed will increase slower than with the square root of time.

It should finally be noticed that all cumulative volumes presented here were calculated by numerical integration (saturation resolution of $1 \cdot 10^{-4}$) of the ED front position profiles vs. distance using the simple trapezoid rule[55].

3. INPUT DATA FOR FAE METHOD TESTING

Four synthetic example cases with typical numerical input values of relative permeabilities and capillary pressure functions for a medium characterized as strongly water-wet (SWW), weakly water-wet (WWW), where gas is non-wetting phase (GAS) and mixed-wettability (MXW) have been created to demonstrate features of the new method. The relative permeability curves emerging from the input parameters for all cases in Table 1 are plotted in Fig. 8 vs. water saturation whereas the capillary pressure functions are plotted in Fig. 9. The water phase is for simplicity assumed mobile in the same water saturation range for all cases, i.e. from 0.2 – 0.68 where 0.68 is assumed to be equal to $1 - S_{or}$ ($1 - S_{gr}$ for the gas case). The capillary pressure, relative permeabilities and non-wetting phase viscosity are varied for the different cases to mimic typical values associated with media being weakly water-wet and mixed-wet. Gas was defined as the non-wetting phase in one case, so the non-wetting phase viscosity of 1 cP typical for oil used for the other cases has been reduced by a factor 1,000 for this case. A discussion of how the method will behave if the highest water saturation obtained in the spontaneous process (S_S) is less than $1 - S_{or}$ is also included in the discussion section.

Finally, the 1-D COUC SI test GVB-3 reported by Bourbiaux and Kalaydjian[12] has been modelled using the new FAE method. The input data given by Bourbiaux and Kalaydjian were parametrized using the same correlations as for the synthetic data and the resulting input values are also included in Table 1. Plots for the corresponding flow functions are shown in Fig. 10. The relative permeability and capillary pressure curves for all cases were parametrized using Brooks - Corey parameters[56] and the Skjæveland correlation (only positive capillary pressure values considered), $P_c = \frac{c_w}{S_w^{a_w}}$, where c_w and a_w are fitting parameters[57], respectively.

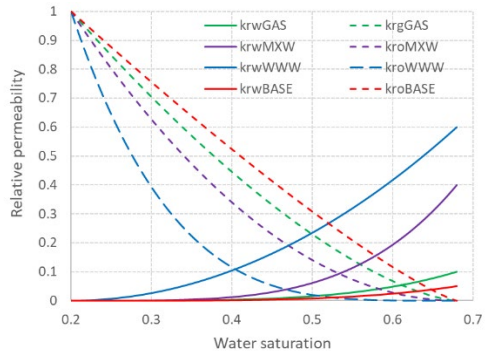

Figure 8. Relative permeability curves in the water saturation range 0.1999 – 0.68 according to values in Table 1 and used as input to the model in the four synthetic cases referred to as SWW, WWW, GAS and MXW.

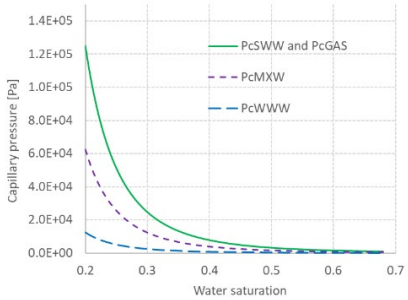

Figure 9. Capillary pressure curves in the water saturation range 0.1999 – 0.68 according to values in Table 1 and used as input to the model in the 3 synthetic cases referred to as SWW, WWW, GAS and MXW.

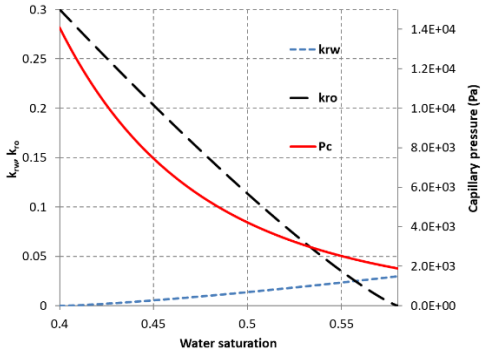

Fig. 10. Counter-current relative permeability and capillary pressure functions in the water saturation range 0.3999 – 0.58 according to values in Table 1 used to model experiment GVB-3 reported by Bourbiaux and Kalaydjian[12].

Table 1. Model input parameters for all synthetic cases together with the input data used to model test GVB-3 reported by Bourbiaux and Kalaydjian[12]. Only the positive part of the capillary pressure curve is used as input when modeling capillary pressure so the negative part in the Skjæveland correlation was neglected by putting $c_o = 0$.

Parameter	SWW	WWW	GAS	MXW	GVB-3
Core length, cm	10	10	10	10	29
Permeability, mD	1,000	1,000	1,000	1,000	124
Porosity (–)	0.22	0.22	0.22	0.22	0.225
Water viscosity, cP	1.0	1.0	1.0	1.0	1.2
Oil or gas viscosity, cP	1.0	1.0	0.001	1.0	1.5
k_{ro} or k_{rg} end-point (–)	1.0	1.0	1.0	1.0	0.3
k_{rw} end-point (–)	0.05	0.6	0.1	0.4	0.03
Corey n_w (–)	4	2	4	4	1.3
Corey n_o or n_g (–)	1.2	4	1.5	2	1.1
S_{wi} (initial) (–)	0.1999	0.1999	0.1999	0.1999	0.3999
S_s (end spontaneous) (–)	0.68	0.68	0.68	0.68	0.58

S_{or} or S_{gr} (residual) (–)	0.32	0.32	0.32	0.32	0.42
c_w (bar)	0.002	0.0002	0.002	0.001	0.001
a_w (–)	4	4	4	4	5.4

4. RESULTS AND DISCUSSIONS

4.1. ED Water Saturation Distances Travelled and Cumulative Water Imbibed vs. Time for Four Synthetic Cases (SWW, WWW, GAS and MXW). The aim in this section is to show how the FAE method can predict cumulative water imbibed vs. time and the propagating water saturation profiles both up to and after the ED shock front contacts the no-flow boundary. The calculations can be performed using a simple spreadsheet. The water saturation profiles (Fig. 5) and construction of the ED shock front water saturation (Fig. 6) can be performed by using eq. (14) whereas cumulative water imbibed can be determined by eq. (16) and (19) for early and late time, respectively. The results are compared to the MS semi-analytical solution which gives the exact value for cumulative water imbibed up to the point when the waterfront contacts the no-flow boundary according to that model formulation.

The FAE method assumes that the diffusion process is independent of water saturation once the capillary diffusion coefficient has obtained its constant value according to the water saturation where it is evaluated ($D(S_{w0})$ is fixed when S_{w0} has been fixed). The results show that this assumption in general leads to an underprediction of cumulative water imbibed in the range from 0 – 24 % for the 4 synthetic cases considered, as compared to the exact MS solution. Since the exact relationship between the approximation used here (constant $D(S_{w0})$) and the correct MS solution is not known, it will for simplicity be assumed that there is a correlation between the shape of the concentration dependent diffusion coefficient (water saturation here) and amount of diffusing substance (water) entering the medium[28]. The correlation proposed assumes that the deviation between the MS solution and the new FAE method when calculating cumulative water imbibed is depending on the value of the normalized water saturation where the capillary diffusion coefficient has its maximum value. A multiplicative correction factor N is introduced based on the four synthetic cases tested and the value of N is given vs. normalized water saturation where the capillary diffusion coefficient has its maximum value, as shown in Fig. 11 and tabulated in Table 2.

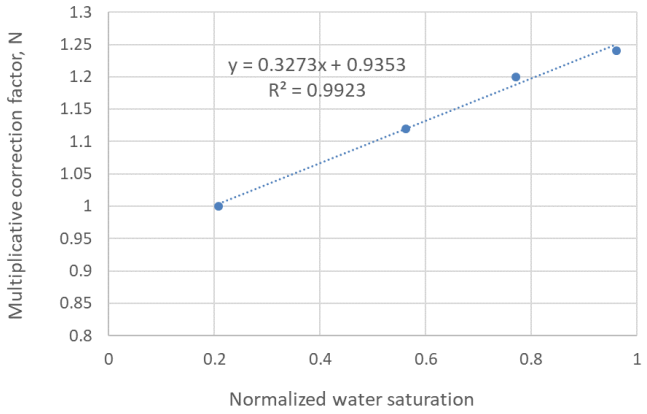

Fig. 11. Multiplicative correction factor N vs. normalized water saturation where the capillary diffusion coefficient has its maximum value.

Table 2. Tabulated data for multiplicative correction factor N and corresponding normalized water saturations for all 4 synthetic cases analyzed (SWW, WWW, GAS and MXW) and used to establish the correlation. The N value for the case GVB-3 is estimated based on the correlation using the normalized water saturation where the capillary diffusion coefficient obtained its maximum value.

Case	Maximum for $D(S_{w0})$ at water saturation	Water saturation at maximum minus initial water saturation	Normalized water saturation	Correction factor N
SWW	0.57	0.37	0.771	1.2
WWW	0.3	0.1	0.208	1
GAS	0.661	0.461	0.96	1.24
MXW	0.47	0.27	0.563	1.12
GVB-3	0.49	0.09	0.5	1.1

It can be observed that the multiplicative correction factor N is increasing the higher the normalized water saturation by which the capillary diffusion coefficient, $D(S_w)$, has its maximum value. Such cases are typical for systems where the medium is characterized as strongly water-wet and or if the viscosity of the non-wetting phase is small compared to the wetting phase viscosity. The correction factor N decreases when the normalized water saturation where the capillary diffusion coefficient has its maximum occurs at medium and lower normalized saturations approaching no correction (N = 1) when the normalized saturation is close to 0.2. Such cases are typical for systems being less water-wet and or if the viscosity of the non-wetting phase is significantly higher than the wetting phase viscosity. It is important to notice that the correction factor correlation in Fig. 11 is purely based on the synthetic input data arbitrarily chosen herein and cannot be expected to be valid for input parameters very different from the ones used here. The correction factor N can, however, always be calculated by the semi-analytical MS solution[7,9].

Considering the SWW case, using the petrophysical data together with the relative permeability and capillary pressure functions from Fig. 8 and 9, ED distributions are shown in Fig. 12 as function of time. The shape of the curves showing x_{ED}^f for the different water saturations at different times, has a maximum for high water saturation, $S_{w0} = 0.57$, typical for parameter values characterizing strongly water-wet conditions. Hence, the maximum value is corresponding to normalized water saturation 0.771 giving a correction factor of N = 1.2 to get the exact value as the MS solution.

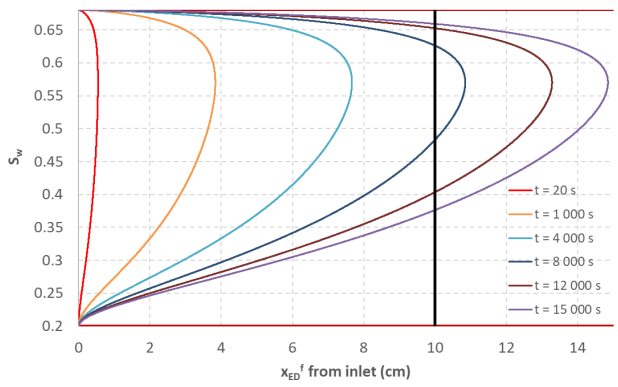

Figure 12. x_{ED}^f curves plotted at different times for water saturation in the range from initial water saturation of 0.1999 to the saturation where SI ceases ($S_s = 0.68$) using the input parameters values for the SWW case given in Table 1. x_{ED}^f is propagating proportionally to square root of time and the correction factor N = 1.2 has been included. The bold black vertical line is representing the no-flow boundary as the porous medium in all synthetic cases is 10 cm long. Hence, the x_{ED}^f values plotted for distances longer than 10 cm are only included for illustration purposes. In the FAE model, the movement of all x_{ED}^f stops at the no-flow boundary (see Fig. 13).

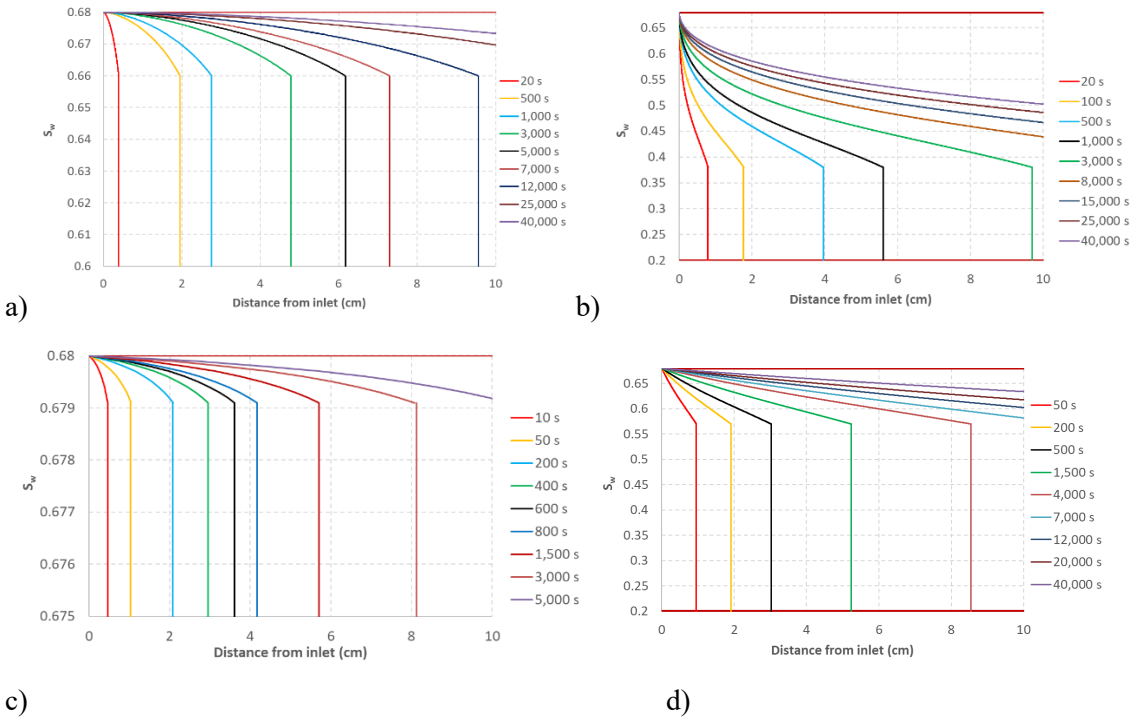

Fig. 13. ED water saturation fronts including shock front for different times vs. distance from inlet face with input values in Table 1 for (a) SWW case with $S_{SF} = 0.66$ and $t_R = 3$ h 48 min. (b) WWW case with $S_{SF} = 0.38$ and $t_R = 53$ min. (c) GAS case with $S_{SF} = 0.679$ and $t_R = 1$ h 27 min. (note the y-axis scale on this plot) and (d) MXW case with $S_{SF} = 0.57$ and $t_R = 1$ h 32 min.

The next key quantity to consider is the shock front water saturation, S_{SF}. It is important because the time required for the water to contact the no-flow boundary is given by the velocity of this water saturation. S_{SF} also gives a measure of the displacement efficiency in line with the conventional BL method. The higher the S_{SF}, the higher the displacement efficiency. S_{SF} is determined by truncate the ED water saturation front profile such that the two shaded areas exemplified and illustrated in Fig. 6 become equal. This will result in an ED shock front water saturation of $S_{SF} = 0.66$ for the SWW case as shown in Fig. 13 (a). The displacement efficiency for this case is hence quite high as expected since it is representing a case being SWW. The time required for the ED shock front saturation to contact the no-flow boundary, t_R, can be estimated using eq. (15) and it is approximately 3 h 48 min. Fig. 13 (b) shows propagation of ED water saturation fronts including the ED shock front vs. time for the weakly water-wet (WWW) case. For such unfavorable displacement conditions, the ED shock front saturation S_{SF} is low, 0.38, so the time for the ED shock front to reach the no-flow boundary is short, $t_R = 53$ min. Fig. 13 (c) shows propagation of ED water saturation fronts including the ED shock front vs. time for the case where gas is replacing oil as the non-wetting phase. For such favorable displacement conditions caused by the very low viscosity of the displaced phase, the ED shock front saturation S_{SF} is very high, 0.679. Hence, the gas displacement process is effectively almost piston-like. It should be noted that the y-axis scale for this case only cover the range 0.675 – 0.68 to be able to distinguish the saturations above the ED shock front saturation. The time required for the ED shock front to contact the no-flow boundary is $t_R = 1$ h 27 min. Fig. 13 (d) shows propagation of ED water saturation fronts including ED shock fronts vs. time for the case described as having mixed-wettability (MXW). The displacement conditions are poorer than for the SWW but still much better than for the WWW case. Hence, the ED shock front saturation S_{SF} is 0.57, and $t_R = 1$ h 32 min.

Cumulative water imbibed vs. time before the ED water shock front contacts the no-flow boundary can be calculated using eq. (14) or just by a simple numerical integration of the area swept by the water saturation profiles in Fig. 13. The latter way will give the same cumulative volume as eq. (14) because the area swept is the same regardless of whether the original water saturation profiles or the truncated shock front profiles are considered. This procedure is not applicable after the shock front

water saturation has contacted the no-flow boundary. Cumulative water imbibed vs. time after the ED water shock front has reached the no-flow boundary must be calculated using eq. (19). The critical quantity regarding this calculation is S^*, i.e. the highest water saturation located exactly at the no-flow boundary. S^* is exactly equal to the ED shock front water saturation S_{SF} when the ED shock front arrives at the no-flow boundary. For times > t_R, the value of S^* is equal to the ED water saturation front value for a given time exactly on the no-flow boundary, i.e. at 10 cm away from the inlet face in all synthetic cases consider here. Hence, cumulative water imbibed vs. time during the post-contact period is therefore equal to the area $A_{CS}(S^* - S_{wi})L_R$ plus the integral of the ED water saturation front profile for saturations above S^*, i.e. $N \cdot A_{CS} \int_{S^*}^{S_s} x_{ED}^f dS_w$. Results for ED shock front water saturation S_{SF}, t_R and cumulative water imbibed as fraction of maximum volume imbibed are summarized in Table 3 for all the cases analyzed herein.

Table 3. ED shock front saturation S_{SF}, time required for the ED shock front to contact the no-flow boundary t_R (including the correction factor N) and cumulative water imbibed as fraction of maximum volume imbibed for all four synthetic cases analyzed together with the data for test GVB-3 reported by Bourbiaux and Kalaydjian[12]. Corresponding data calculated using the MS semi-analytical solution is given in brackets for each case whenever relevant.

Case	Shock front water saturation, S_{SF} [fraction]	Time to reach no-flow boundary, t_R (eq. (17))	Cumulative water imbibed at t_R [fraction of maximum = fractional recovery] (eq. (14))
SWW	0.66	13,700 s ≈ 3 h 48 min (4,430 s = 1 h 13 min)	0.97 (0.6)
WWW	0.38	3,200 s ≈ 53.3 min (587 s = 9.7 min)	0.55 (0.22)
GAS	0.679	5,200 s ≈ 1 h 27 min (1,978 s = 33 min)	0.999 (0.63)
MXW	0.57	5,500 s ≈ 1 h 32 min (1,638 s = 27.3 min)	0.8 (0.48)
GVB-3	0.54	300,000 s = 83 h 20 min	0.93

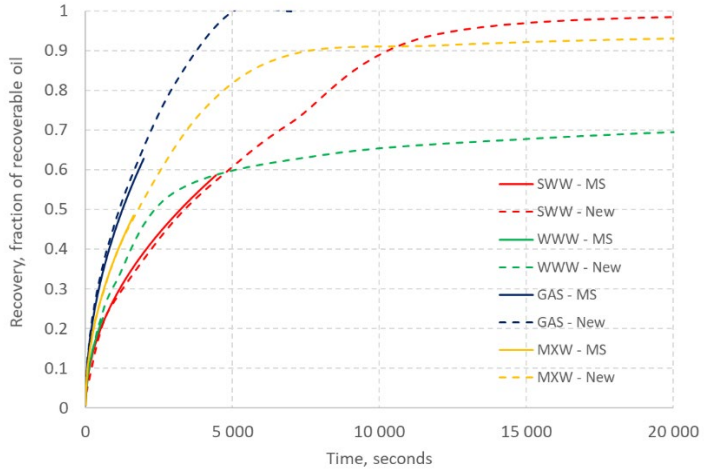

Fig. 14. Cumulative water imbibed as fraction of maximum volume imbibed vs. time for all the synthetic cases using the FAE method compared to the MS semi-analytical solution for equal input values specified in Table 1. The FAE and MS methods shows very good agreement before the imbibing

water contacted the no-flow boundary for all cases (SWW, WWW, GAS and MXW) when correction factors of N = 1.2, 1, 1.24 and 1.12 were used, respectively. The MS solutions are plotted until the imbibing water contacts the no-flow boundary as it is not valid beyond that time. Since the FAE method is valid for all times, it can predict the entire process.

Cumulative water imbibed as fraction of maximum volume imbibed (or fractional recovery of oil) vs. time is plotted in Fig. 14 for all synthetic cases SWW, WWW, GAS and MXW together with corresponding data calculated using the MS semi-analytical solution. The latter curves (lines) end when the waterfront contacts the no-flow. The correspondence between the exact semi-analytical MS method and the new methodology is perfect due to the use of correction factors N = 1.2, 1, 1.24 and 1.12, respectively, until the MS solution ceases to be valid. That happens at $t_R = 4{,}430$ s for the SWW case in red when the fractional recovery is approximately 0.6. The new FAE method is, however, predicting a t_R of 13,700 s (3 h 48 min.) with a corresponding fractional recovery of approximately 0.97, red broken curve. The general shape of the fractional recovery curve vs. time after the ED shock front has contacted the no-flow boundary is additionally qualitatively corroborated by many experimental studies reported in the literature[2,11-19,24-26]. Corresponding plots for the MS and new FAE method for the WWW case are shown in green, respectively. The MS and FAE solutions have t_R of about 10 and 53 min., respectively, with corresponding fractional recoveries of 0.22 and 0.55. It can be observed that the time required to approach fractional recovery of unity will be extremely long caused by the unfavorable curvature of the ED water saturation fronts above the ED shock front. (Fig. 13 (b)). Corresponding plots for the MS and new FAE method for the GAS case are shown in blue, respectively. The MS and FAE solutions have t_R of about 0.5 and 1.5 h, respectively, with corresponding fractional recoveries of 0.63 and 0.999. It can be observed that the displacement efficiency is very high caused by the favorable mobility ratio between low viscous gas and water, (Fig. 13 (c)). Corresponding plots for the MS and new FAE method for the MXW case are shown in yellow, respectively. The MS and FAE solutions have t_R of about 0.5 and 1.5 h, respectively, with corresponding fractional recoveries of 0.48 and 0.8. Hence, the displacement efficiency is quite good, although smaller than for the SWW case but significantly higher than the WWW case.

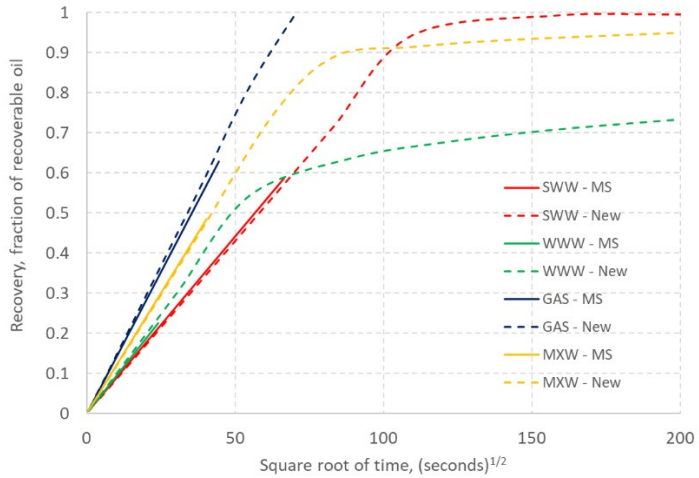

Fig. 15. Cumulative water imbibed as fraction of maximum volume imbibed vs. square root of time for the SWW, WWW, GAS and MXW cases using the new FAE method and the MS semi-analytical method with equal input values given in Table 1. Correction factors of N = 1.2, 1, 1.24 and 1.12 were used, respectively. The MS solutions are plotted until the imbibing water contacts the no-flow boundary according to that model formulation.

The point in time when the imbibing ED shock front contacts the no-flow boundary can be visualized even clearer in Fig. 15, where fractional recoveries for all synthetic cases instead are plotted vs. square root of time. The ED water shock front contacts the no-flow boundary exactly when the fractional recovery is deviating from a straight line at a fractional recovery of about 0.97 for the SWW case (red broken), equivalent to a square root of time of 117 $s^{1/2}$. Numbers for the WWW case (green broken) are fractional recovery of 0.55 equivalent to square root of time of 57 $s^{1/2}$. For the GAS case (blue broken) the numbers are fractional recovery of 0.999 equivalent to square root of time of 72 $s^{1/2}$. The MXW case has fractional recovery of 0.8 (yellow broken) equivalent to square root of time of 74 $s^{1/2}$.

To summarize, it seems that the new FAE method is corroborated quantitatively regarding cumulative water imbibed up to and after the imbibing water has contacted the no-flow boundary. That is based on a qualitative and visual comparison between the calculated fractional recovery curves vs. time and typical expected behavior for such curves based on experimental tests reported in the literature. It is also important to note the significant difference between the new FAE formulation and the MS solution regarding the time, t_R, required for the water front to contact the no-flow boundary. More testing should be performed using empirical data and measured input values to distinguish the ability of the two formulations to corroborate high-quality empirical data.

4.5. ED Water Saturation Distances Travelled and Cumulative Water Imbibed vs. Time for the Cases GVB-3. There are not many complete sets in the literature addressing 1-D COUC SI where all input data is measured and available to perform a quantitative comparison between measured data and model predictions. An exception is the highly cited paper by Bourbiaux and Kalaydjian[12]. The focus here will be test GVB-3 which was performed in 1-D COUC flow mode on a sandstone rock sample from Vosges, France. The sample was paralleled piped with a cross-section area of 6.1x2.1 cm^2 and length of 29 cm (no-flow boundaries on the lateral sides). The absolute permeability was 124 mD and the porosity 0.225. Relative permeability and capillary pressure curves used to generate predictions for cumulative water imbibed using the FAE method were those presented in Fig. 10 with corresponding input parameter values in Table 1. So-called counter-current relative permeability values were used by the authors when simulating the COUC experimental data. Counter-current relative permeabilities as shown in Fig. 10 were therefore also used as input to the FAE method when calculating cumulative water volume imbibed. So-called COUC relative permeabilities is a concept introduced to account for the observed lower fractional recovery rate in COUC SI tests compared to co-current SI tests. The physical argument for introducing COUC relative permeability curves is based on that momentum transfer between two immiscible fluids is depending on whether the fluids are moving co- or counter currently[58,59]. Since the magnitude and impact this effect may have on the individual water and oil relative permeability curves, the concept of COUC relative permeabilities adds uncertainty when such processes are simulated. The choice used by Bourbiaux and Kalaydjian[12] was to reduce the measured water and oil co-current relative permeability curves with the same factor (= 0.7) when used to simulate COUC processes.

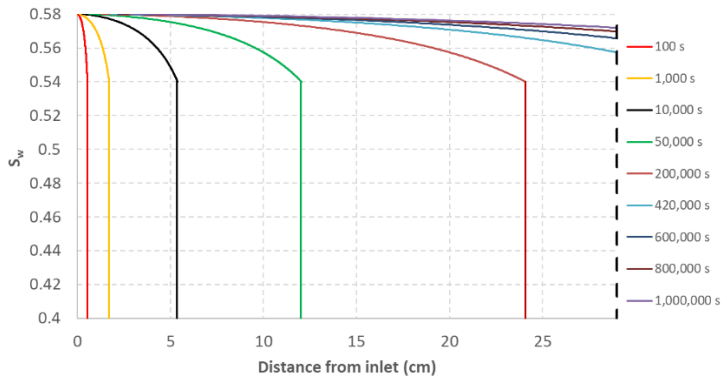

Fig. 16. ED water saturation profiles including ED shock front for different times vs. distance from inlet face for the GVB-3 case with input values in Table 1 reported by Bourbiaux and Kalaydjian[12]. A

correction factor of N = 1.1 was used based on the correlation in Fig. 12. The ED shock front saturation is $S_{SF} = 0.54$ and time to reach the no-flow boundary $t_R = 83$ h 20 min.

Fig. 16 shows the ED water saturation profiles including the ED shock front for the GVB-3 test. The mobile water saturation range is from 0.4 – 0.58 and the ED shock front saturation 0.54. Since the new FAE method is valid for all times, it can predict fractional recovery of non-wetting phase up to the end of the process as shown in Fig. 17, although with a small discrepancy between experimental and the case called New for late times. It should be noticed that a correction factor of N = 1.1 was used here based on the correlation depicted in Fig. 11. The small deviation between fractional recovery for the FAE method developed and the experimental data is assumed to be caused by the lack of an appropriate parametrization of the capillary pressure curve in the vicinity of the highest water saturation, S_S. If the capillary pressure curve is manually adjusted in the vicinity of S_S, a fractional recovery curve as indicated as New modified appears. Hence, if the deviation between the observed fractional recovery curve and the curve calculated using the FAE method is ascribed to uncertainties in the capillary pressure curve, the new modified curve shows that it is possible to close the discrepancy between measured fractional recovery and the FAE method results at high water saturation by adjusting the capillary pressure curve slightly in this saturation region. The data provided by Bourbiaux and Kalaydjian[12] in their Fig. 12 indicates some uncertainty in the measured capillary pressure data. It therefore seems, based on a comparison between the experiment GVB-3 and the FAE results, that they are equal within the experimental uncertainty in the input parameters. Hence, the main hypothesis put forward here related to establishment of a FAE also for COUC flow cannot be falsified by comparing its consequences with the only available complete experimental input dataset in the literature.

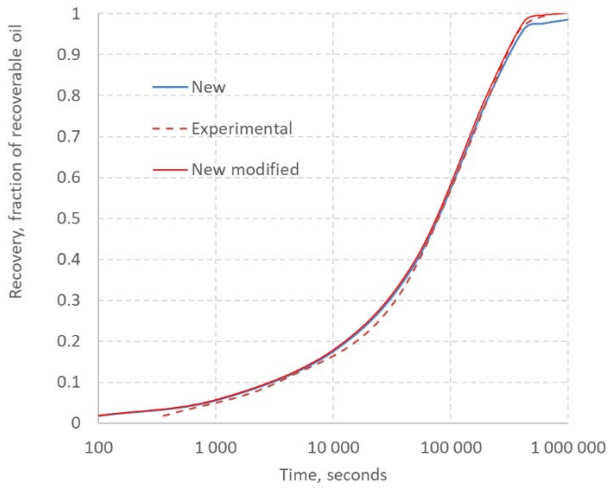

Fig. 17. Cumulative water imbibed as fractional recovery of non-wetting phase vs. time for the GVB-3 case using input values in Table 1. The FAE method shows very good agreement with the experimental data (a correction factor of N = 1.1 was used based on the correlation in Fig. 11). Since the FAE method is valid for all times, it can predict fractional recovery of non-wetting phase until the end of the process, although with a small discrepancy between experimental and FAE method result for late times close to fractional recovery of unity.

4.6. Discussion of the Approach Developed and Other Consequences. The new FAE method is based on the use of constant diffusion coefficients for each water saturation in the mobile saturation range in eq. (9). The use of constant diffusion coefficients is necessary to obtain an analytical expression for the FAE (eq. (14)) where the relationship between all parameters is clearly shown. But since the original partial differential equation (eq. (1)) is nonlinear, calculating cumulative water imbibed from combining

the contributions of individual saturations, S_{w0}, is deviating slightly from the correct value as calculated by the MS semi-analytical scheme. Hence, a correction factor N was calculated and correlated linearly with the normalized saturation where the diffusion coefficient peaks. This factor is suggested to be included in the expression for cumulative water volume imbibed in eq. (16) and (19). There is, however, still uncertainty related to whether the correction factor should be applied with equal weight for all ED water saturation fronts because the impact the nonlinearity of the capillary diffusion coefficient vs. water saturation has on cumulative water imbibed is not known. Several examples demonstrated that it could be important is included e.g. by Crank[28], Chapter 9. In eq. (16) and (19), all water saturations are multiplied with the same factor N. If different weight factor should be used for different water saturations depending on the shape of the capillary diffusion coefficient, it could give plots for ED fronts different from that in Fig. 5 and the ED shock front saturation, S_{SF} could be shifted from the one obtained using equal N for all water saturations.

It was assumed in all the synthetic cases studied herein, for simplicity, that the highest water saturation during the SI process, S_S, was identical to the residual oil saturation $(1 - S_{or})$ after a subsequent forced imbibition. This can be a valid assumption when working with rock material characterized as strongly water-wet. If, however, the wettability of rock samples tends toward less water-wet condition, a significant difference between S_S and the residual oil saturation $(1 - S_{or})$ after forced imbibition normally appears. The SI process ceases when there are no gradients in the chemical potential inside the medium and the pressure in the wetting phase is equal in bulk and inside the porous medium, even when the capillary diffusion coefficient has a finite value > 0 at the water saturation where that condition occurs, i.e. S_S. That is typically occurring when the wettability of the actual medium is not strongly water-wet. For the type of analysis performed here, it implies that the highest water saturation characteristic occurring during the spontaneous process, S_S, will be mobile and move slowly to the right proportional to square root of time. Except that, the procedures for estimating ED shock front saturation, cumulative water imbibed vs. time etc. remain that same as previously described. The SI process will theoretically cease when the highest water saturation, S_S, has travelled the length of the rock sample.

The underlying phenomenon for describing diffusion on the microscopic level used herein is Brownian motion theory[42-44]. This framework is also widely applied elsewhere for modeling of processes and phenomena in mathematics, physics, biology and economy (e.g. stock market price fluctuations). Standnes[60] also recently used Brownian motion theory to derive a modified version of Darcy's law for variation of absolute permeability for changes in system temperature. Being in line with the basic physical principles, the framework applied herein may potentially possess additional possibilities for extending current approaches and methods applied when describing multiphase flow in porous media.

As a final note, it is a requirement in all empirical sciences that theoretical models are tested against experimental data. Since only one complete dataset was found in the literature, a challenge exists regarding available high-quality complete datasets for testing of 1-D COUC SI models. Experimentalists are therefore strongly encouraged to generate more complete high-quality datasets whose absence represents a constraint for further theoretical advancements related to the phenomenon 1-D counter-current spontaneous imbibition of water into porous media.

5. CONCLUSIONS

A new method is developed for interpretation and quantification of 1-D counter-current (COUC) spontaneous imbibition (SI) processes based on a hypothesis that microscopic theory for diffusion can be combined with the solution of the diffusion equation to establish a frontal advance equation (FAE) for such processes as well. The FAE method assumes the use of constant diffusion coefficients for each water saturation when calculating the equivalent distance front travelled by each saturation vs. time, which induces a deviation from the correct value for cumulative water imbibed vs. time. The deviation can easily be corrected for by including a correction factor N in the range 1.0-1.24 based on a comparison with the exact solution given by McWhorter and Sunada (1990). The following conclusions can be drawn from this work:

- The new FAE method (visual and easy-to-use) is in line with the Buckley – Leverett method for forced imbibition and therefore valid for times both before and after the imbibing water phase contacts the no-flow boundary. It gives:
    - Cumulative water imbibed or fractional recovery of non-wetting phase vs. time before and after the water contacts the no-flow boundary
    - Time required for the equivalent distance water shock front to propagate through the medium to the no-flow boundary
    - The spatial development of water saturation in the porous medium throughout the whole process
    - Quantification of the above-mentioned measurable quantities with no additional input data required compared to the conventional methods used to model 1-D COUC SI processes
- The results obtained using the FAE cannot be falsified within the experimental uncertainty based on a comparison with the GVB-3 test reported by Bourbiaux and Kalydijan (1990)
    - It is furthermore corroborated qualitatively (typical water saturation in the porous medium when imbibing water contacts the no-flow boundary and the slow increase in water saturation in the post-contact period) by four synthetic cases tested herein as well as results from numerous 1-D COUC SI experiments published in the literature

The FAE method developed seems like a very promising method to analyze 1-D COUC SI processes. More testing is encouraged to further support its applicability for a wider set of experimental input data.

ACKNOWLEDGEMENTS

The corresponding author acknowledges Equinor ASA for supporting external activities as adjunct professor positions.

ABBREVIATIONS

A	Constant in the McWhorter and Sunada model
A_{CS}	Cross-sectional area of porous medium or reservoir
a_w	Parameter in the Skjæveland correlation
BL	Buckley – Leverett
C	Proportionality constant
COUC	Counter-current
c_w	Parameter in the Skjæveland correlation
$D(S_{w0})$	Capillary diffusion coefficient evaluated at water saturation S_{w0}
D_M	Diffusion coefficient
ED	Equivalent distance (x_{ED})
ET	Early time
f	Fractional flow according to Buckley - Leverett
$F(S_w)$	Fractional flow of water according to McWhorter and Sunada
FAE	Frontal advance equation
$G(S_w) = \frac{2}{\sqrt{\pi}}\sqrt{D(S_{w0})t}$	Proportionality factor to describe the relationship between distance and square root of time
GVB-3	Test reported by Bourbiaux and Kalydijan

K	Absolute permeability
k_{rg}	Relative permeability to gas
k_{ro}	Relative permeability to oil
k_{rw}	Relative permeability to water
L_R	Length of porous medium
LT	Late time
MS	McWhorter and Sunada
MXW	Mixed wettability
N	Correction factor to bring the solution in line with the MS solution
n_g	Corey exponent to gas
n_o	Corey exponent to oil
n_w	Corey exponent to water
P_c	Capillary pressure
Q_w	Cumulative water
q	Water injection rate
q_w	Water flux
R_{ET}	Recovery, early time
R_{LT}	Recovery, late time
R_{V_ET}	Recovery in volume, early time
R_{V_LT}	Recovery in volume, late time
SI	Spontaneous imbibition
SWW	Strongly water-wet
S_{gr}	Residual gas saturation
S_{or}	Residual oil saturation
S_s	Water saturation after spontaneous imbibition
S_{SF}	Water shock front saturation
S_w	Water saturation
S_{wi}	Initial water saturation
S^*	Water saturation on the no-flow boundary
t	Time
t_R	Time required for the water to arrive at the no-flow boundary
x	Distance
x_{ED}	Equivalent distance (ED)
x_{ED}^f	Equivalent distance front
WWW	Weakly water-wet
ϕ	Porosity

μ_o	Oil viscosity
μ_w	Water viscosity

REFERENCES

1) Abd, A.S.; Elhafyan, E.; Siddiqui, A.R.; Alnoush, W.; Blunt, M.J.; Al Yafei, N. A review of the phenomenon of counter-current spontaneous imbibition: Analysis and data interpretation. *Journal of Petroleum Science and Engineering*, **2019**, 180, 456 - 470. https://doi.org/10.1016/j.petrol.2019.05.066
2) Mason, G.; Morrow, N.R. Developments in spontaneous imbibition and possibilities for future work, *Journal of* Petroleum *Science and Engineering*, **2013**, 110, 268 – 293.
3) Meng, Q.; Liu, H.; Wang, J. A critical review on fundamental mechanisms of spontaneous imbibition and the impact of boundary condition, fluid viscosity and wettability, *Advances in Geo-Energy Research*, **2017**, 1(1), 1 – 17.
4) March, R.; Doster, F.; Geiger, S. Accurate early-time and late-time modeling of countercurrent spontaneous imbibition, *Water Resources Research*, **2016**, 52, 6263 – 6276, doi:10.1002/2015WR018456.
5) Nooruddin, H.A.; Blunt, M.J. Analytical and numerical investigations of spontaneous imbibition in porous media, *Water Resources Research*, **2016**, 52(9), 7284 – 7310.
6) Schmid, K.S.; Geiger, S. Universal scaling of spontaneous imbibition for water-wet systems, *Water Resources Research*, **2012**, 48(3), W03507.
7) Schmid, K.S.; Geiger, S. Universal scaling of spontaneous imbibition for arbitrary petrophysical properties: Water-wet and mixed-wet states and Handy's conjecture, *Journal of Petroleum Science and Engineering*, **2013**, 101, 44 – 61.
8) Schmid, K.S.; Alyafei, N.; Geiger, S.; Blunt, M.J. Analytical Solutions for Spontaneous Imbibition: Fractional-Flow Theory and Experimental Analysis, *SPEJ*, **2016**, 21(6), 2308 – 2317.
9) McWhorter, D.B.; Sunada, D.K. Exact integral solutions for two-phase flow, *Water Resources Research*, **1990**, 26(3), 399 – 413.
10) McWhorter, D.B. Infiltration affected by flow of air, HYDROLOGY PAPERS COLORADO STATE UNIVERSITY, **1971**, Fort Collins, Colorado.
11) Arabjamaloei, R.; Ruth, D.W.; Mason, G.; Morrow, N.R. Solutions for counter-current spontaneous imbibition as derived by means of a similarity approach, *Journal of Porous Media*, **2015**, 18(2), 113 – 124.
12) Bourbiaux, B.J.; Kalaydjian, F.J. Experimental Study of Cocurrent and Countercurrent Flows in Natural Porous Media. SPE RE, **1990**, 5(3), 360 – 374.
13) Cuiec, L.E.; Bourbiaux, B.J.; Kalaydjian, F.J. Oil Recovery by Imbibition in Low-Permeability Chalk. *SPEFE*, **1994**, 9(3), 200-208.
14) Hamon, G.; Vidal, J. Scaling-up the capillary imbibition process from laboratory experiments on homogeneous and heterogeneous samples, European Petroleum Conference, **1986**, SPE 15852.
15) Hatiboglu, C.U.; Babadagli, T. Experimental and visual analysis of co- and counter-current spontaneous imbibition for different viscosity ratios, interfacial tensions, and wettabilities, *Journal of Petroleum Science and Engineering*, **2010**, 70, 214 – 228.
16) Morrow, N.R.; Mason, G. Recovery of oil by spontaneous imbibition. *Current Opinion in Colloid and Interface Science,* **2001**, 6(4), 321 – 337.
17) Alyafei, N.; Blunt, M.J. Estimation of relative permeability and capillary pressure from mass imbibition experiments, *Advances in Water Resources*, **2018**, 115, 88 – 94.
18) Handy, L.L. Determination of Effective Capillary Pressures For Porous Media from Imbibition Data, *Petroleum Transactions, AIME*, **1960**, 219, 75 – 80.
19) Li, Y.; Morrow, N.R.; Ruth, D. Similarity solution for linear counter-current spontaneous imbibition, *Journal of Petroleum Science and Engineering*, **2003**, 39, 309 – 326.
20) Rangel-German, E.R.; Kovscek, A.R. Experimental and analytical study of multidimensional imbibition in fractured porous media, *Journal of Petroleum Science and Engineering*, **2002**, 36 (1–2), 45 – 60.

21) Akin, S.; Schembre, J.M; Bhat, S.K.; Kovscek, A.R. Spontaneous imbibition characteristics of diatomite, *Journal of Petroleum Science and Engineering*, **2000**, 25, 149 – 165.

22) Alyafei, N.; Al-Menhali, A.; Blunt, M.J. Experimental and Analytical Investigation of Spontaneous Imbibition in Water-Wet Carbonate, *Transport in Porous Media*, **2016**, 115(1), 189 – 207.

23) Le Guen, S.S.; Kovscek, A.R. Nonequilibrium Effects During Spontaneous Imbibition, *Transport in Porous Media*, **2006**, 63, 127 – 146.

24) Li, Y.; Ruth, D.; Mason, G.; Morrow, N.R. Pressures acting in counter-current spontaneous imbibition, *Journal of Petroleum Science and Engineering*, **2006**, 52, 87 – 99.

25) Ruth, D.W.; Li, Y.; Mason, G.; Morrow, N.R. An Approximate Analytical Solution for Counter-Current Spontaneous Imbibition, *Transport in Porous Media*, **2007**, 66(3), 373 – 390.

26) Zhang, S.; Pu, H.; Zhao, X. Experimental and Numerical Studies of Spontaneous Imbibition with Different Boundary Conditions: Case Study of Middle Bakken and Berea Cores, *Energy and Fuels*, **2019**, 33(8), 5135 – 5146.

27) Bjørnarå, T.I.; Mathias, S.A. A pseudospectral approach to the McWhorter and Sunada equation for two-phase flow in porous media with capillary pressure, *Computational Geoscience*, **2013**, 17(6), 889 – 897.

28) Crank, J. The mathematics of diffusion, 2nd Edition, **1975**, Oxford University Press.

29) Schmid, K.S.; Geiger, S.; Sorbie, K.S. Semianalytical solutions for cocurrent and countercurrent imbibition and dispersion of solutes in immiscible two-phase flow, *Water Resources Research*, **2011**, 47(2), W02550.

30) Knight, J.H.; Philip, J.R. Exact solutions in nonlinear diffusion, *J. Eng. Math.*, **1974**, 8(3), 219 - 227.

31) Reis, J.C.; Cil, M. A Model for Oil Expulsion by Countercurrent Water Imbibition in Rocks: One-Dimensional Geometry. *Journal of Petroleum Science & Engineering*, **1993**, 10, 97.

32) Tavassoli, Z.; Zimmerman, R.W; Blunt, M.J. Analysis of counter-current imbibition with gravity in weakly water-wet systems, *Journal of Petroleum Science and Engineering*, **2005**, 48 (1–2), 94–104.

33) Yortsos, Y.C.; Fokas, A.S. An analytical solution for linear waterflood including the effects of capillary pressure, *SPEJ*, **1983**, 23(1), 115 – 124.

34) Behbahani, H.S.; Di Donato, G.; Blunt, M.J. Simulation of counter-current imbibition in water-wet fractured reservoirs, *Journal of Petroleum Science and Engineering*, **2006**, 50, 21 – 39.

35) Pooladi-Darvish, M.; Firoozabadi, A. Cocurrent and Countercurrent Imbibition in a Water-Wet Matrix Block, *SPEJ*, **2000**, 5(1), 3 – 11.

36) Kashchiev, D.; Firoozabadi, A. Analytical solutions for 1-D countercurrent imbibition in water-wet media, *SPEJ*, **2002**, 8(4), 401– 408.

37) Silin, D.; Patzek, T. On Barenblatt's Model of Spontaneous Countercurrent Imbibition. *Transport in Porous Media*, **2004**, 54, 297 – 322.

38) Buckley, S.E.; Leverett, M.C. Mechanism of fluid displacements in sands, *Transactions of the AIME,* **1942**, 146, 107 – 116.

39) Hauge, E.H. Forelesninger i Teoretisk fysikk II B. Institutt for teoretisk fysikk NTH, **1970**.

40) Foley, A.Y.; Nooruddin, H.A.; Blunt, M.J. The impact of capillary backpressure on spontaneous counter-current imbibition in porous media, *Advances in Water Resources*, **2017**, 107, 405 – 420.

41) Bear, J. Dynamics of Fluids in Porous Media. *Dover publications, Inc*., **1972**.

42) Brown, R. A brief account of microscopical observations made in the months of June, July and August 1827, on the particles contained in the pollen of plants; and on the general existence of active molecules in organic and inorganic bodies. *Philosophical Magazine,* **1828**, 4, 161 – 173.

43) Einstein, A. Über die von der molekularkinetischen Theorie der Wärme geforderte Bewegung von in ruhenden Flüssigkeiten suspendierten Teilchen, *Annalen der Physik*, **1905**, 17, 549 – 560.

44) Lemons, D.S.; Gythiel, A. Paul Langevin's 1908 paper ''On the Theory of Brownian Motion'' ['' Sur la the´orie du mouvement brownien,'' C. R. Acad. Sci. (Paris) 146 530–533 (1908)]. *Am. J. Phys*, **1997**, 65, 11, 1079 – 1081.

45) Li, Y.; Mason, G.; Morrow, N.R.; Ruth, D. Capillary pressure at the imbibition front during water–oil counter-current spontaneous imbibition, *Transport in Porous Media*, **2009**, 77(3), 475–487.

46) Li, Y.; Mason, G.; Morrow, N.R.; Ruth, D. Capillary pressure at a Saturation Front During Restricted Counter-Current Spontaneous Imbibition with Liquid Displacing Air, *Transport in Porous Media*, **2011**, 87(3), 275 – 289.

47) Morel-Seytoux, H.J. Two-Phase Flow in Porous Media, in *Advances in Hydroscience*, 9th Ed., R.J.M. Dewiest (ed.), **1973**, Academic Press, San Diego, California.

48) Kleppe, H. Buckley – Leverett Theory, Lecture notes PET565 Core Scale Modeling and Interpretation Part A, **2017**, University of Stavanger, Norway.

49) Akin, S.; Kovscek, A.R. Imbibition Studies of Low-Permeability Porous Media, **1999**, SPE paper 54590.

50) Baldwin, B.A.; Spinler, A. In-situ saturation development during spontaneous imbibition, *Journal of Petroleum Science and Engineering*, **2002**, 35, 23 – 32.

51) Fernø, M.A.; Haugen, Å.; Wickramathilaka, S.; Howard, J.; Graue, A.; Mason, G.; Morrow, N.R. Magnetic resonance imaging of the development of fronts during spontaneous imbibition, *Journal of Petroleum Science and Engineering*, **2013**, 101, 1 – 11.

52) Føyen, T.L. Onset of spontaneous imbibition, Master thesis, Department of Physics and Technology, **2016**, University of Bergen Norway.

53) Zhou, D.; Jia, L.; Kamath, J.; Kovscek, A.R. Scaling of counter-current imbibition processes in low-permeability porous media, *Journal of Petroleum Science and Engineering*, **2002**, 33(1–3), 61 – 74.

54) Wickramathilaka, S.; Howard, J.J.; Stevens, J.C.; Morrow, N.R.; Mason, G.; Haugen, Å.; Graue, A.; Fernø, M. Magnetic resonance imaging of oil recovery during spontaneous imbibition from cores with two-ends open boundary conditions, Paper SCA2011-24 presented at the Society of Core Analysts meeting Austin, Texas, U.S.A., 18 – 21 Sept., **2011**.

55) Edwards, C.H. Jr.; Penney, D.E. Calculus and Analytical Geometry, Prentice-Hall, Inc., Englewood Cliffs, **1982**, New Jersey.

56) Brooks, R.H.; Corey, A.T. Hydraulic Properties of Porous Media, Hydrology Papers 3, **1964**, Colorado State University, Fort Collins.

57) Skjaeveland, S.M.; Siqveland, L.M.; Kjosavik, A.; Hammervold Thomas, W.L.; Virnovsky, G.A. Capillary Pressure Correlation for Mixed-Wet Reservoirs, *SPE REE*, **2000**, 3(1), 60 – 67.

58) Qiao, Y.; Andersen, P.Ø.; Evje, S.; Standnes, D.C. A Mixture Theory Approach to Model Co- and Counter-Current Two-Phase Flow in Porous Media Accounting for Viscous Coupling. *Advances in Water Resources,* **2018**, 112, 170 – 188.

59) Standnes, D.C.; Andersen, P.Ø. Analysis of the Impact of Fluid Viscosities on the Rate of Counter-Current Spontaneous Imbibition. *Energy and Fuels,* **2017**, 31*,* 6928 –6940.

60) Standnes, D.C. Implications of Molecular Thermal Fluctuations on Fluid Flow in Porous Media and Its Relevance to Absolute Permeability, *Energy and Fuels*, **2018**, 32(8), 8024 – 8039.